International Journal of GEOMATE, Feb., 2023, Vol.24, Issue 102, pp.18-25
ISSN: 2186-2982 (P), 2186-2990 (O), Japan, DOI: https://doi.org/10.21660/2023.102.g12141
Geotechnique, Construction Materials and Environment

SOIL BEHAVIOR MODELING BY MPS-CAE SIMULATION

Sudip Shakya [1] and * Shinya Inazumi [2]

[1] Graduate School of Engineering and Science, Shibaura Institute of Technology, Japan;
[2] College of Engineering, Shibaura Institute of Technology, Japan

*Corresponding Author, Received: 10 May 2022, Revised: 10 Jan. 2023, Accepted: 26 Jan. 2023

ABSTRACT: Many numerical simulation methods have been developed in the current research field. The authenticity of the simulation-based research depends on the accuracy of the model prepared. The modeling of the soil becomes challenging when there is the presence of water and the soil starts behaving like a fluid. This study focuses on the application of the MPS (moving particle semi-implicit) - CAE (computer-aided engineering) method to design the setup for the unconfined compression test to determine the correct parameters of the soil model. The soil material is assumed to be Bingham fluid and will be employed as a bi-viscosity model, where the soil particle exists at both rigid and fluid states depending upon the condition. The best-fitting soil model was designed for the primary parameters and is compared with the benchmark soil data to justify the claim. Furthermore, the authors endeavored to find the secondary governing factors that will affect the accuracy of the soil modeling. The results show that the values of the primary parameters are influenced by the values of the secondary parameters, resulting in a different model. The influence of the secondary parameters was studied, and the best-fitting soil model was designed by incorporating both primary and secondary parameters. The resultant soil model is expected to provide more accurate results if used as a reference in various construction simulations.

Keywords: Moving particle semi-implicit, Computer-aided engineering, Parameter fitting, Soil modeling, Unconfined compressive strength

1. INTRODUCTION

The simulation-based research works are popular in the current academic society, especially for complex and expensive topics to conduct and evaluate in real life. In the field of geotechnical engineering, these kinds of research are conducted to study soil behavior and soil-improvement methods and to visualize and evaluate construction phenomena. Many numerical simulation methods have been developed in the field of geotechnical engineering. Numerical simulations in the field of geotechnical engineering are generally carried out from the design phase of the soil model and adjust the specifications to the designed model for generating the desired output. One of such numerical simulation method is an MPS-CAE simulation. The MPS-CAE simulation incorporates the moving particles semi-implicit (MPS method) as the numerical analysis method.

The accuracy of numerical simulations mostly depends on the accuracy of the model created. Depending upon the type of numerical simulation, the method of analysis and the analysis condition adopted in the numerical simulation differs. For example, when there is the presence of water in the numerical simulation, analysis methods like the finite element method (FEM), discrete element method (DEM), etc., cannot analyze the influence of water, but MPS method can simulate the fluid behavior by using the equations of the motion of the fluid. However, MPS method assumes all participating materials as a fluid and soil particles are not ideal fluid. Therefore, unlike other participating materials, the governing parameters for the soil are difficult to measure and cannot be appropriately modeled for simulation.

Inazumi et al. [1] used an unconfined compression test simulation to check the validity of the soil parameters employed in the visualization and evaluation of jet grouting technology. Shakya et al [2] used the generalized material parameters generated from the unconfined compression test to produce realistic jet grouting simulation results.

This study focuses on the application of a computer-aided engineering (CAE) system that simulates the performance of soil-improvement methods and to visualize and evaluate soil behavior. Specifically, the paper attempts to establish the reverse calculation method determining the soil parameters for the MPS-CAE simulation by conducting the MPS-CAE simulation on unconfined compression test. The primary governing parameters that define the soil models in the MPS-CAE simulation are the plastic viscosity, yield value, and yield parameter. These governing parameters are initially inputted as input values and simulated to find the output result. Through the

attempt, the authors propose a method to perform soil behavior modeling by MPS-CAE simulation with high accuracy. These achievements contribute to establish the reliability and effectiveness of MPS-CAE simulation in the field of geotechnical engineering.

2. MPS-CAE SIMULATION

2.1 CAE and MPS Method

Computer-aided engineering (CAE) [4-8] refers to the technology that helps to simulate and analyze large-scale construction experiments from the various stages using the prototypes on a computer. These prototypes are created by CAD (computer-aided design) and others, considering the surrounding conditions [4-8]. In the field of geotechnical engineering, CAE can be used to visualize the inside of the soil and the stress acting on the inside of the soil, and to understand experiments that would require huge costs and/or phenomena that would be difficult to reproduce. In addition, by performing appropriate post-processing, it is possible to communicate with other people in a visually easy-to-understand manner

Moving particles semi-implicit (MPS) is one of the numerical simulation methods to analyze the behavior of the fluid particles according to the equations of the motion of fluid. The governing equations for the incompressible flow used in the analysis are the mass conservation law of Eq. (1) and the Navier's stroke law of Eq. (2) considering surface tension.

$$\frac{D\rho}{Dt} = 0 \tag{1}$$

$$\frac{Du}{Dt} = -\frac{1}{\rho}\nabla P + \vartheta\nabla^2 u + g + \frac{1}{\rho}\sigma k\delta n \tag{2}$$

where, ρ is the density of the fluid, u is the velocity vector, P is the pressure, ϑ is the kinematic viscosity coefficient, g is the gravity vector, σ is the surface tension coefficient, k is the curvature, δ is the delta function for the surface tension to act on the surface, and n is the unit vector in the direction perpendicular to the surface.

In the MPS method, each differential operator (slope, divergence, and Laplacian) of the governing equation, as shown in Eq. (2), is discretized by a weighting function [1-4]. The weighting function depends on each particle interaction model's interparticle distance r and the influence radius (R: 2.1 to 4.1 times the interparticle distance).

The weighting function (w) is expressed by Eq. (3), and its a function of the distance (r) between particles and the influence radius (R) of the support domain.

$$w(r) = \begin{cases} \frac{R}{r} - 1 & (0 \le r \le R) \\ 0 & (R \le r) \end{cases} \tag{3}$$

The sum of the weight functions in the support domain is commonly known as the particle number density (n_i) and it is defined as Eq. (4).

$$n_i = \sum_{j \neq i} w_{ij} \tag{4}$$

Where, $\boldsymbol{w_{ij} = w(r_{ij}, R)}$ is the weight function between particle ($\boldsymbol{i}$) and ($\boldsymbol{j}$). The particle number density when particles are located on a regular grid whose grid size is the same with the diameter of the particles is called the criterion of particle number density ($\boldsymbol{n^*}$).

In the derivative models for the traditional MPS method, the differential operators for the gradient, Laplacian, and divergence of a particle ($\boldsymbol{i}$) are formulated as Eqs. (5) to (7).

$$< \nabla_{\emptyset} >_i = \frac{d}{n^*}\sum_{j \neq i} \frac{\emptyset_{ij}}{r_{ij}^2} x_{ij} w_{ij} \tag{5}$$

$$< \nabla_{\emptyset}^2 >_i = \frac{2d}{n^* \lambda_i}\sum_{j \neq i} \emptyset_{ij}\, w_{ij} \tag{6}$$

$$< \nabla . \Phi >_i = \frac{d}{n^*}\sum_{j \neq i} \frac{\emptyset_{ij} . x_{ij}}{r_{ij}^2} w_{ij} \tag{7}$$

Where, $\emptyset$ is an arbitrary scalar, $\boldsymbol{\Phi}$ is an arbitrary vector, and $\boldsymbol{\lambda}$ is a coefficient in the Laplacian model which is defined as Eq. (8).

$$\bar{\lambda_i} = \frac{\sum_{j \neq i} w_{ij}\, r_{ij}^2}{\sum_{j \neq i} w_{ij}} \tag{8}$$

2.2 Fluid Model

A Bingham fluid is a fluid that begins to flow only when the shear stress exceeds a yield stress value, otherwise remains stationary. Therefore, until the shear stress exceeds the yield stress value, it is regarded as being in a rigid state. But, the analysis becomes impossible for the fluid model with strain rate of 0, so the model employed for this fluid is a bi-viscosity model [1], [2] as shown in Fig. 1. It treats the fluid as a viscoplastic fluid in the fluid state, and as a highly-viscous fluid in a rigid state.

The apparent viscosity in the fluid state is reflected in Eq. (9).

$$\eta = \left(\eta_p + \frac{\tau_y}{\dot{\gamma}}\right) \tag{9}$$

The apparent viscosity in the rigid state is reflected in Eq. (10).

$$\eta = \left(\eta_p + \frac{\tau_y}{\dot{\gamma}}\right) \quad (10)$$

Where, $\boldsymbol{\tau_y}$ is the yield value, $\boldsymbol{\eta_p}$ is the plastic viscosity, $\dot{\boldsymbol{\gamma}}$ is the average shear velocity, and $\dot{\boldsymbol{\gamma}}_{\boldsymbol{c}}$ is the yield criterion of the fluid and rigid states, given by Eq. (11).

$$\dot{\gamma}_c = \frac{2C_y\,\tau_y}{\eta_p} \quad (11)$$

Where, $\boldsymbol{C_y}$ is the yield parameter.

During the design stage, the yield value ($\boldsymbol{\tau_y}$), plastic viscosity ($\boldsymbol{\eta_p}$), and yield parameter ($\boldsymbol{C_y}$) are presented as the model parameters. These parameters will be termed as the primary parameters in the later part.

3. SIMULATION CONDITION

3.1 Modelling and Specification

Figure 2 shows the model setup for the unconfined compression test. A cylindrical soil sample of 50×100 mm was sandwiched between two metallic plates of 10 mm in height each. These models are designed by CAD software and imported into the MPS-CAE method. The bottom plate remains stationary, but the top plate will be lowered such that the soil will deform at the constant strain ratio of 1% per minute, recreating the mechanism of the compression machine. It was simulated for a total time of 1200 seconds, during which the soil was expected to exceed the yield value.

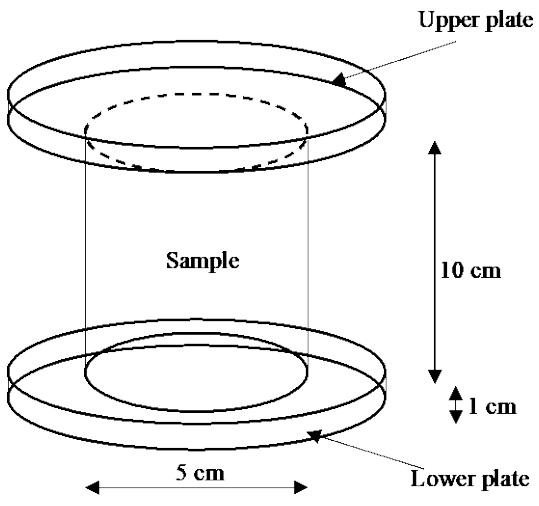

Fig. 2 Unconfined compression test model

The effects of the yield value, plastic viscosity, and yield parameters were studied for soil with a strength level of 60 kPa and subjected to numerous trial-and-error simulations. In this way, the best-fitting soil model was designed. The yield value was inputted as 60 kPa and the values of the other parameters, at which the input yield value became equal to the output yield value, were determined.

3.2 Material Parameters

Table 1 shows the final values of the materials parameters that produced the best-fitting stress-strain curve in the unconfined compression test. The soil material was assumed to be Bingham fluid, whereas water was a Newtonian fluid. These values are selected after numerous trial-and-error simulations incorporating the different values of the primary parameters. The input value for the yield value was kept constant in each simulation, i.e., 60 kPa, and the value of plastic viscosity and yield parameter at which the output yield value matches the input yield value was determined. The values were selected in such a way that the simulation itself becomes successful, i.e., there is a chance of the simulation sample behaving like fluid and flowing during the compression test. In such cases, the output results will not be generated. During this phase, the effect of density was not studied in detail, and the common density value was selected. It was assumed that the influence of surface tension was negligible in this simulation due to the lack of sufficient water content in the sample soil. The assumption was found legitimate when it was studied in detail later.

4. RESULTS

4.1 Comparison of Results with Known Data

Figure 3 shows the results of the simulated stress-strain curve compared with the two known data when the Table 1 data was inputted. The simulated soil sample yielded at a compressive strength of 61.24 kN/m^2 and a strain value of 12.59%. The soil was assumed to be 3 mm sized for this simulation, which usually lies in the sand category in a real-life scenario. In a simulation, the calculation load is directly proportional to the total number of particles. Depending upon the input value of soil particle size, the number of the particles is determined, so the larger soil diameter was inputted to reduce the calculation load.

Meanwhile, the soil size of the two known data was smaller but was used as the benchmark for comparison in this study. The Aomori soil sample was silty soil with an average diameter of 0.0036 mm. It is represented by the rectangular plotted points. It has a dry density value of 793 kg/m^3 and

Table 1 Material parameters

Material	Density (kg/m^3)	w/c	Yield value (Pa)	Plastic viscosity (Pa.s)	Yield parameter (-)	Surface tension (N/m)	Fluid model
Water	1000	-	-	-	-	0.10	Newtonian fluid
Ground	1600	-	60000	17000	0.0001	0.002	Bingham fluid

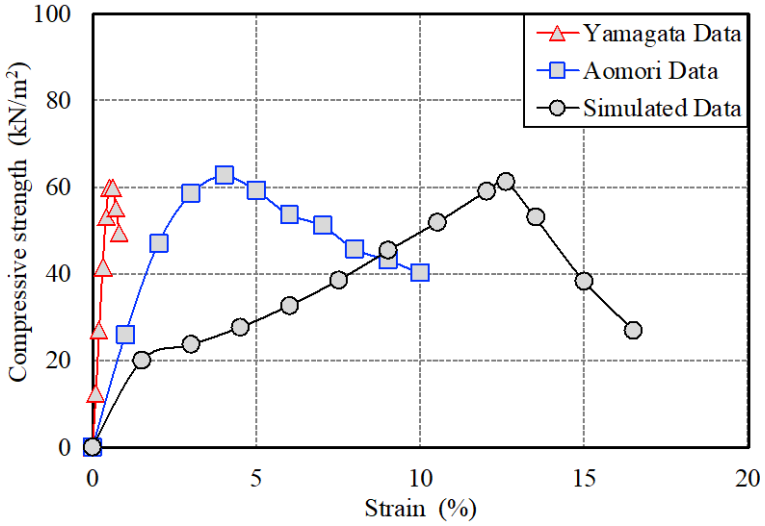

Fig. 3 Simulation results compared to known data

a water content of 86.5%. It yielded at a compressive strength of 64.69 kN/m^2 and a strain value of 4.73%. The Yamagata soil sample, represented by the triangular plotted points, was sandy soil with an average soil diameter of 0.034 mm. It has a dry density value of 1172 kg/m^3 and a water content of 46.8%. It yielded at a compressive strength of 61.55 kN/m^2 and a strain value of 0.55%. The input value for the simulation data compared to the benchmark data differed only in density and soil particle size. The soil density varies for each sample depending on various factors like water content, depth of excavation sampling, soil composition, etc. As for the result, the peak strength of the simulation results and benchmark data are approximately equal, but they all yielded at different strain values. To determine the cause of this discrepancy, further study was conducted with the objective of determining the secondary parameters.

4.2 Influence of Density and Soil Particle Size

In this simulation, the soil particles were assumed to be Bingham fluid, but the soil particles are not an ideal fluid. It assumes the soil particles to be 100% fluid but exists at two different states and possess the same density in all cases. However, the density of soil changes depending on the water content and other reasons. The simulation method did not have detailed configuration settings for the water content, but there is a configuration setting for the density, which is inputted as the input parameter. Since the water content of the soil sample could not be defined clearly, the input value for density was changed numerous times for the same simulations while keeping all other parameters constant. The results showed that the values for the output compressive strength and exerted strain were almost the same, implying that the change in density does not affect the soil model design if the yield value, yield parameter, surface tension, and plastic viscosity are kept constant in each simulation. Table 2 summarizes the overall simulation results for the changing density.

Since the benchmark data have different particle sizes and generate different strain values, the study was conducted to determine the influence of the particle size in the simulation. Figure 4 shows the changes in the stress-strain curve's characteristics when the particle size in the simulation was changed to 2, 1, and 0.5 mm compared to that of 3-mm soil particles. Like the case study of density variation, all the other parameters were kept the same. The results showed drastic changes in both output yield value and strain value. The yield value increased for the smaller soil particles. The increase for the 2-mm soil particles was low and almost negligible but it was remarkable for the 1-mm and 0.5-mm soil particles. Meanwhile, the strain value decreased remarkably for the smaller soil particles. The

Table 2 Influence of density of ground modelling

Yield value = 60 kPa, Plastic viscosity = 17000 Pa·s,	Density (kg/m^3)	Compressive strength (kN/m^2)	Strain (%)
Particle size = 3 mm,	1600	61.299	12.59
Yield parameter = 0.0001,	1172	61.559	12.49
Surface tension = 0.002 N/m	793	61.702	12.4

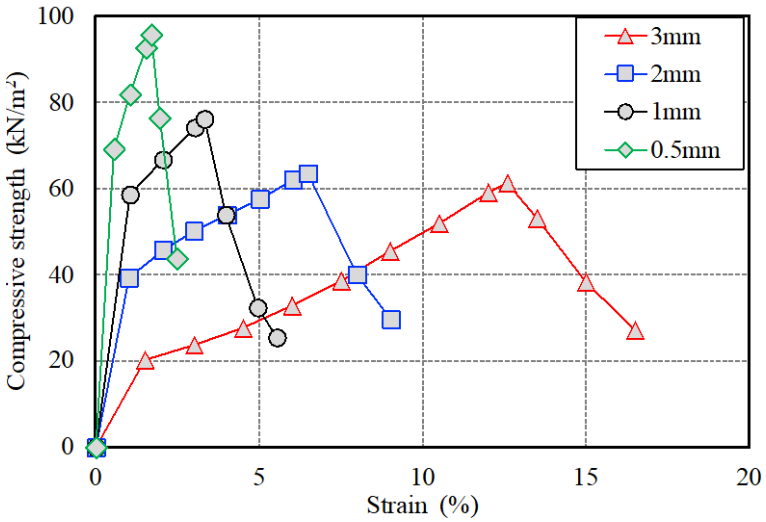

Fig. 4 Comparison of simulated results for particles of various sizes

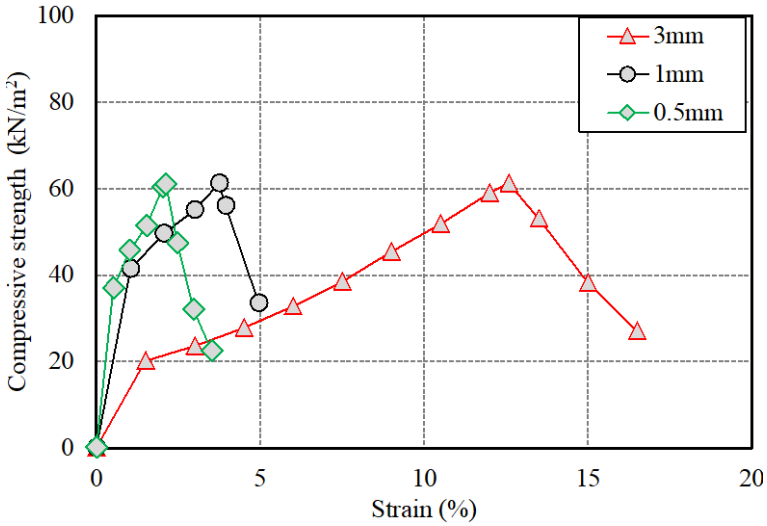

Fig. 5 Correct output model for 0.5-mm and 1-mm soil particles

decrease in the strain value is approximately 50% for each consecutive soil size. The soil samples yielded at 63.43, 76.03, and 95.54 kN/m^2, respectively, and the strain values of 6.48, 3.34, and 1.69%, respectively.

4.3 Remodeling for Different Soil Particle Sizes

Since the influence of the secondary parameters has been quantified, a correct model was designed for each soil particle size. The objective was to match the output where the yielding occurs at approximately 60 kPa·same as the yielding value of benchmark data. This process included numerous trial-and-error simulations in determining the accurate values of the primary parameters, similar to the methodology in the initial phase.

Figure 5 shows the correct stress-strain

Table 3 New material parameters and output results for each soil particle size

Soil size (mm)	Input yield value (Pa)	Plastic viscosity (Pa·s)	Yield parameter (-)	Output yield value (kPa)	Strain (%)	Fluid model
3	60000	17000	0.0001	61.30	1.26	Bingham fluid
1	60000	10000	0.0001	61.30	0.38	Bingham fluid
0.5	60000	5500	0.0001	61.07	0.21	Bingham fluid

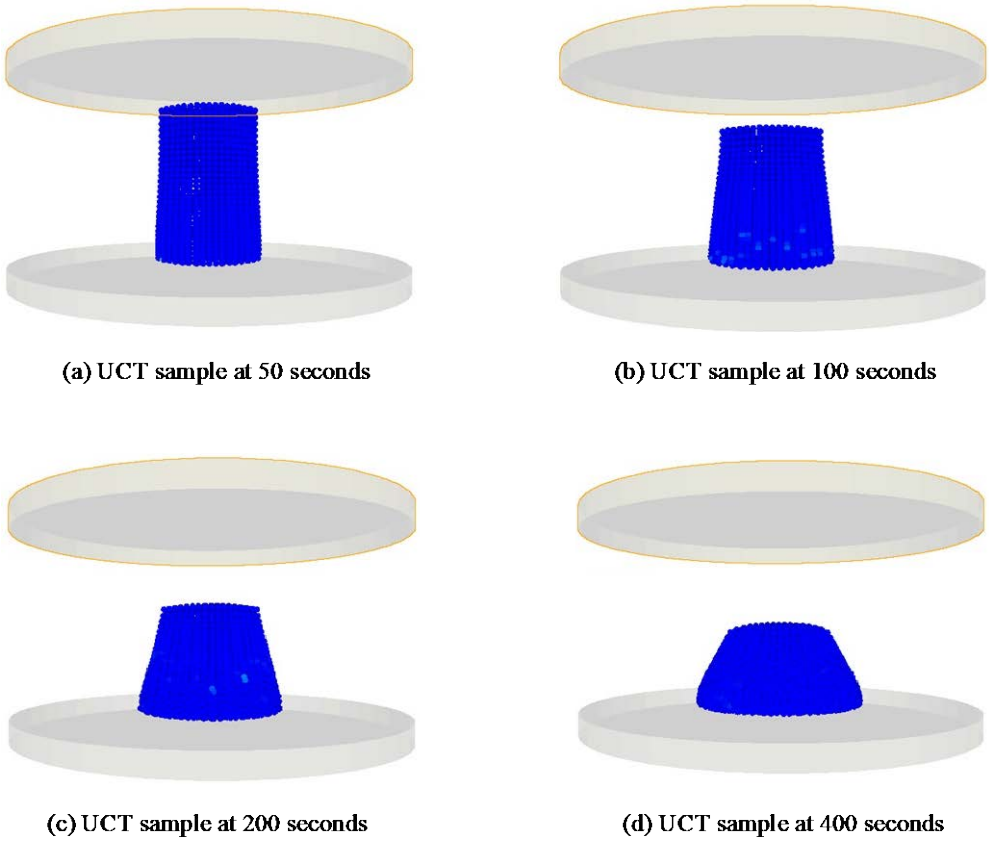

(a) UCT sample at 50 seconds

(b) UCT sample at 100 seconds

(c) UCT sample at 200 seconds

(d) UCT sample at 400 seconds

Fig. 6 Collapse of the UCT sample due to wrong parameter settings

relationship for soil particles of sizes 0.5 mm and 1 mm compared to the 3-mm soil particles. Since the secondary parameter did not influence the yielding value for the 2-mm soil particles compared to the yielding benchmark yielding value, it was not remodeled in this study. This study's interest lies in remodeling the finer soil particles, which showed more deviation from the original 3-mm soil particles. However, if the situation demands, it can be remodeled for fine-tuned results.

Table 3 shows the details of the new soil parameters and output values for each soil particle size. For the 0.5-mm soil particles, the output compressive strength of 61.07 kN/m^2 and strain value of 2.11% were obtained for the input plastic viscosity of 5500 Pa·s. For the 1-mm soil particles, the output yield value was recorded as 61.30 kN/m^2, which yielded a strain value of 3.76%. These results were obtained for the plastic viscosity of 10000 Pa·s.

5. DISCUSSION

It was observed that the plastic viscosity and strain value for finer soil particles decreased when the yield value and yield parameter were kept constant. The most probable reason for it might lie in the change from the coarse sand category to the fine sand category. Yield value is directly proportional to the plastic viscosity, and assuming the influence factor of the soil composition during the simulation sample formation, it is likely that the finer particles form a more compact bond than the coarse-grained soil particles if both samples are of equal strength. Therefore, it can be speculated that each soil particle has to be of higher strength to

possess the strength equivalent to the strongly bonded simulation sample, implying the possession of higher yield strength and, thus, higher plastic viscosity. Similarly, soil composition might be the key to explaining the change in strain value. The coarse-grained test sample has sufficient voids to allow the excess strain before collapsing.

As for the values selected for the simulation as the best fitting stress-strain curve generating data, appropriate reasoning was placed in each data. For the plastic viscosity, the bi-viscosity model was employed for the simulation where both rigid and fluid states exist. It means that the value of the plastic viscosity should be very high to arrest the fluidity properties. However, the actual values of plastic viscosity can only be speculated by the empirical method based on the simulation results. Likewise, the yield parameter value was selected after the best-fitting scenario was created. The simulation failed for the value greater than 1/1000 as the sample undergoes immediate collapse and does not resemble the unconfined compression test. Figure 6 shows the example of simulation sample collapsing during the trial and error simulation. Also, the value of the yield parameter is likely to be smaller, as suggested by the equations of the bi-viscosity fluid model. When simulated, the influence of the surface tension was found to be low. Thus, its value was assumed to be approximately zero in order to reduce the calculation load. Moreover, since changes in density were seen to have a negligible influence, the soil samples were assumed to be in a dry state, so the value for the surface tension could be neglected.

Simulations for finer soil particles involve an astronomical calculation load and may even fail to produce the results of the unconfined compression test simulation depending upon the calculation load. The calculation duration can be decreased for the finer particles since it will yield at a lower strain value. However, the number of particles will increase and interact with each other more, generating more calculation load. It is necessary to find the optimum size and simulation duration to achieve the most realistic result for soil modeling possible. The next concern is the adaptability of generated model to the other simulation research. For large simulations, the model of smaller soil particles might not be the correct option as it might fail due to the astronomical calculation load. The objective of this study is to create a soil model as accurate as possible such that it can be used as a reference for future studies. Unless powerful simulation method are developed, it might compel to use of the lesser accurate soil model or limit the scope of study in a future study. The same goes for the study of soil modeling as well, since this study has only been able to generate the result for 0.5-mm sized soil particles, which are the size of the sand rather than the soil.

6. CONCLUSIONS

In this study, the soil of 60 kPa·strength was successfully modeled, assuming it follows the behavior of Bingham fluid by employing a bi-viscosity model. The design parameters were initially set to yield value, yield parameters, and plastic viscosity. After determining the influence of the soil size particles, the correct model was designed, incorporating both primary and secondary parameters. It was found that the density and surface tension of the soil had negligible influence on the soil modeling. In this study, the unconfined compression test was successfully established as the reverse calculation method for determining the correct soil parameters by generating the output result equivalent to the input values. However, the challenge for future study remained, regardless of successfully establishing the proper methodology for modeling soil. Unless a more powerful simulation method is developed, the future simulation must always be compromised either in the simulation scope or a more accurate soil model due to the astronomical calculation time and calculation load generated by the presence of a higher particle number. In conclusion, this study will be a helpful reference for future studies related to soil simulations and for creating more accurate soil models.

7. REFERENCES

[1] Inazumi S., Shakya S., Komaki T. and Nakanishi Y., Numerical analysis on performance of middle-pressure jet grouting method for ground improvement, Geosciences, Vol. 11, Issue 8, 2021, 313.

[2] Shakya S., Inazumi S. and Nontananandh S., Potential of computer-aided engineering in the design of ground improvement technologies, Applied Sciences, Vol. 12, Issue 19, 2022, 9675.

[3] Inazumi S., Kuwahara S., Jotisankasa A. and Chaiprakaikeow S., MPS-CAE simulation on dynamic interaction between steel casing and existing pile when pulling out existing piles, International Journal of GEOMATE: Geotechnique, Construction Materials and Environment, Vol. 18, Issue 70, 2020, pp. 68-73.

[4] Nakao K., Inazumi S., Takaue T., Tanaka S. and Shinoi T., Evaluation of discharging surplus soils for relative stirred deep mixing methods by MPS-CAE analysis, Sustainability, Vol. 14, Issue 1, 2022, 58.

[5] Inazumi S., Jotisankasa A., Nakao K. and Chaiprakaikeow S., Performance of mechanical agitation type of ground-improvement by CAE

system using 3-D DEM, Results in Engineering, Vol. 6, 2020, Article: 100108.

[6] Nakao K., Inazumi S., Takahashi T. and Nontananandh S., Numerical simulation of the liquefaction phenomenon by MPSM-DEM coupled CAES, Sustainability, Vol. 14, Issue 12, 2020, 7517.

[7] Inazumi S., Tanaka S., Komaki T. and Kuwahara S., Evaluation of effect of insertion of casing by rotation on existing piles, Geotechnical Research, Vol. 8, Issue 1, 2021, pp. 25-37.

[8] Nakao K., Inazumi S., Takaue T., Tanaka S. and Shinoi T., Visual evaluation of relative deep mixing method type of ground-improvement method, Results in Engineering, Vol. 10, 2021, Article: 100233.